

Resonant LLC Converter: Operation and Design

250W 33Vin 400Vout Design Example

Sam Abdel-Rahman
Infineon Technologies North America (IFNA) Corp.

Resonant LLC Converter: Operation and Design

Sam Abdel-Rahman

Published by Infineon Technologies North America
27703 Emperor Blvd, suite 310
Durham, NC 27703
All Rights Reserved.

Attention please!

THE INFORMATION GIVEN IN THIS APPLICATION NOTE IS GIVEN AS A HINT FOR THE IMPLEMENTATION OF THE INFINEON TECHNOLOGIES COMPONENT ONLY AND SHALL NOT BE REGARDED AS ANY DESCRIPTION OR WARRANTY OF A CERTAIN FUNCTIONALITY, CONDITION OR QUALITY OF THE INFINEON TECHNOLOGIES COMPONENT. THE RECIPIENT OF THIS APPLICATION NOTE MUST VERIFY ANY FUNCTION DESCRIBED HEREIN IN THE REAL APPLICATION. INFINEON TECHNOLOGIES HEREBY DISCLAIMS ANY AND ALL WARRANTIES AND LIABILITIES OF ANY KIND (INCLUDING WITHOUT LIMITATION WARRANTIES OF NON-INFRINGEMENT OF INTELLECTUAL PROPERTY RIGHTS OF ANY THIRD PARTY) WITH RESPECT TO ANY AND ALL INFORMATION GIVEN IN THIS APPLICATION NOTE.

Information

For further information on technology, delivery terms and conditions and prices please contact your nearest Infineon Technologies Office (www.infineon.com).

Warnings

Due to technical requirements components may contain dangerous substances. For information on the types in question please contact your nearest Infineon Technologies Office. Infineon Technologies Components may only be used in life-support devices or systems with the express written approval of Infineon Technologies, if a failure of such components can reasonably be expected to cause the failure of that life-support device or system, or to affect the safety or effectiveness of that device or system. Life support devices or systems are intended to be implanted in the human body, or to support and/or maintain and sustain and/or protect human life. If they fail, it is reasonable to assume that the health of the user or other persons may be endangered.

AN 2012-09

V1.0 September 2012

Author: Sam Abdel-Rahman

We Listen to Your Comments

Any information within this document that you feel is wrong, unclear or missing at all? Your feedback will help us to continuously improve the quality of this document. Please send your proposal (including a reference to this document) to: [Sam.Abdel-Rahman@infineon.com]

Table of contents

| | | |
|----------|--|-----------|
| 1 | Introduction..... | 4 |
| 2 | Overview of LLC Resonant Converter..... | 4 |
| 3 | Design Steps..... | 8 |
| 4 | Bridge and Rectifier Selection | 11 |
| 5 | Design Example..... | 13 |
| 6 | Schematics and Bill of Material | 17 |
| 7 | References | 19 |

1 Introduction

While a resonant LLC converter has several desired features such as high efficiency, low EMI and high power density, the design of a resonant converter is an involved task, and requires more effort for optimization compared to PWM converters. This document aims to simplify this task, and make it easier to optimally design the resonant tank. This document provides an overview of LLC converter operation and design guidelines. Finally, a comprehensive design example is given along with schematics, bill of materials, experimental results and waveforms.

2 Overview of LLC Resonant Converter

This section offers an overview of the LLC converter operation and waveforms in the different modes. Figure 2.1 shows a Full-Bridge LLC converter with Full-Bridge rectifier. In a simplistic discussion, the switching bridge generates a square waveform to excite the LLC resonant tank, which will output a resonant sinusoidal current that gets scaled and rectified by the transformer and rectifier circuit, the output capacitor filters the rectified ac current and outputs a DC voltage.

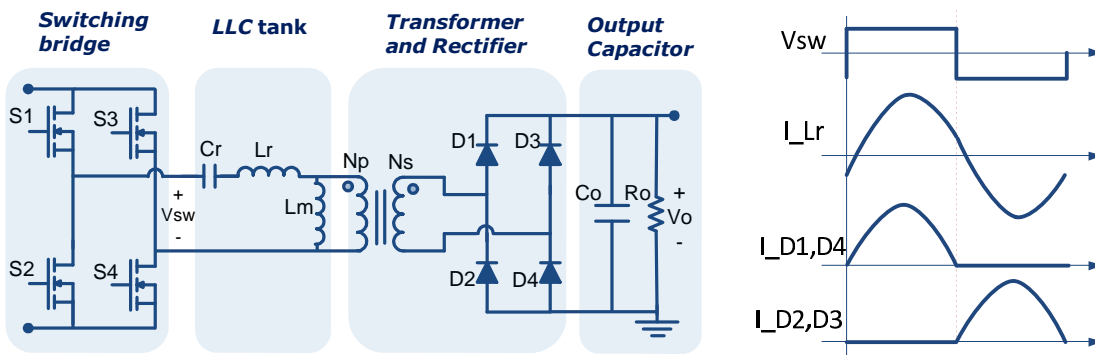


Figure 2.1 Full-Bridge LLC converter with Full-Bridge rectifier

2.1 Converter Voltage Gain

$$\text{Converter gain} = \text{switching bridge gain} * \text{resonant tank gain} * \text{transformer turn ratio (Ns/Np)}$$

Where the switching bridge gain is 1 for a Full-Bridge and 0.5 for a Half-Bridge.

The resonant tank gain can be derived by analyzing the equivalent resonant circuit shown in Figure 2.2, the resonant tank gain is the magnitude of its transfer function as in Eq. 1.

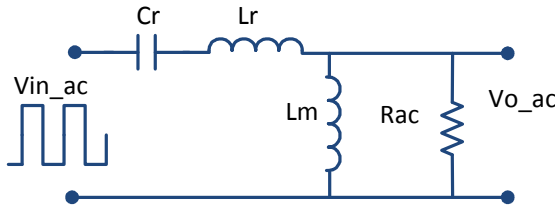


Figure 2.2 Equivalent resonant circuit

$$K(Q, m, F_x) = \left| \frac{V_{o_ac}(s)}{V_{in_ac}(s)} \right| = \frac{F_x^2(m-1)}{\sqrt{(m \cdot F_x^2 - 1)^2 + Fx^2 \cdot (F_x^2 - 1)^2 \cdot (m-1)^2 \cdot Q^2}} \quad \text{Eq. 1}$$

Where,

$$Q = \frac{\sqrt{L_r/C_r}}{R_{ac}} \quad \text{Quality factor}$$

$$R_{ac} = \frac{8}{\pi^2} \cdot \frac{N_p^2}{N_s^2} \cdot R_o \quad \text{Reflected load resistance}$$

$$F_x = \frac{f_s}{f_r} \quad \text{Normalized switching frequency}$$

$$f_r = \frac{1}{2\pi\sqrt{L_r \cdot C_r}} \quad \text{Resonant frequency}$$

$$m = \frac{L_r + L_m}{L_r} \quad \text{Ratio of total primary inductance to resonant inductance}$$

One can plot the resonant tank gain K with the normalized switching frequency for different values of Quality factor Q and any single value of m, as shown in Figure 2.3. The selection of the m value will be discussed in a later section of this document, but m=6 was used as an example.

It can be seen in Figure 2.3 that low Q curves belong to lighter load operation while higher Q curves represent heavier loads. It's also seen that all Q curves (load conditions) cross at the resonant frequency point (at $F_x=1$ or $f_s=f_r$) and have a unity gain.

Figure 2.3 shows that all gain curves has peaks which define the boundary between the inductive and capacitive impedances of the resonant tank, hence we can define the inductive and capacitive operation regions as shaded in the plot, the objective of defining both regions is because it is desired to maintain an inductive operation across the entire input voltage and load current ranges, and never fall into the capacitive region operation. Such requirement is due to that Zero Voltage Switching (ZVS) is only achieved in the inductive region, in addition to that capacitive operation means that current leads the voltage, so the current in the MOSFET will reverse direction before the MOSFET turns off, then after the MOSFET turns off the reverse current will flow in the MOSFET's body diode, which will cause a body diode hard commutation once the other MOSFET in the bridge turns on, which in turn will cause reverse recovery losses and noise, and might cause high current spikes and device failure. The capacitive operation can be prevented and will be discussed in a later section of this document.

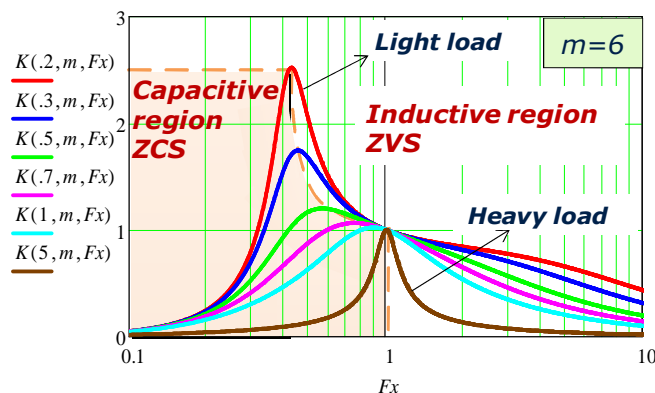


Figure 2.3

2.2 Modes of Operation

Since the LLC network gain is frequency modulated, the converter can operate in three modes depending on input voltage and load current conditions, as listed below and shown in Figure 2.4:

1. At resonant frequency operation, $f_s = f_r$.
2. Above resonant frequency operation $f_s > f_r$.
3. Below Resonant frequency operation, $f_s < f_r$.

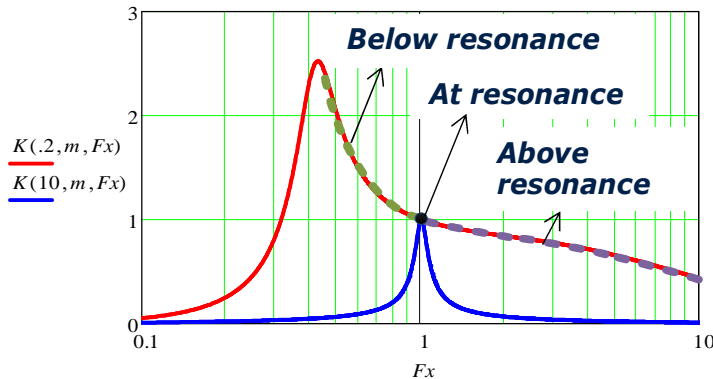


Figure 2.4

Despite the aforementioned three modes; which will be explained in details later in this section; the converter has only two possible operations within the switching cycle, as described below. And each of the modes pointed out above may contain one or both of these operations.

- 1) Power delivery operation, which occurs twice in a switching cycle; first, when the resonant tank is excited with a positive voltage, so the current resonates in the positive direction in the first half of the switching cycle, the equivalent circuit of this mode is shown in Figure 2.5, and second occurrence is when the resonant tank is excited with negative voltage, so the current resonates in the negative direction in the second half of the switching cycle, the equivalent circuit of this mode is shown in Figure 2.6.

During the power delivery operations, the magnetizing inductor voltage is the positive/negative reflected output voltage and the magnetizing current is charging/discharging respectively.

The difference between the resonant current and the magnetizing current passes through the transformer and rectifier to the secondary side, and power is delivered to the load.

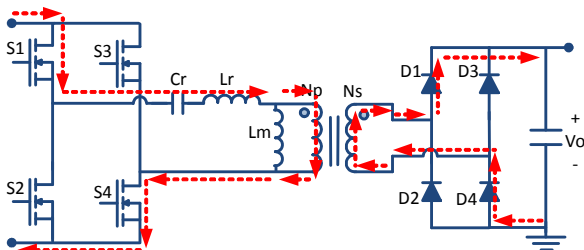


Figure 2.5

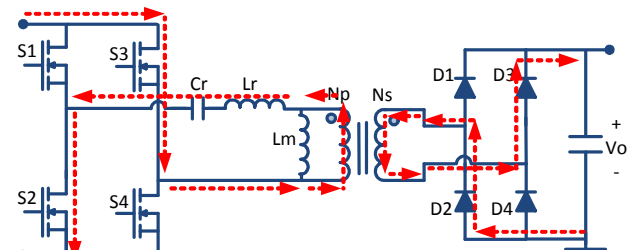


Figure 2.6

- 2) Freewheeling operation, which can occurs following the power delivery operation only if the resonant current reaches the transformer magnetizing current, this only happens when $f_s < f_r$, causing the transformer secondary current to reach zero and the secondary side rectifier to disconnect, consequently the magnetizing inductor will be free to enter the resonance with the resonant inductor and capacitor, the frequency of this second resonance is smaller than the original resonant frequency f_r , especially at high values of m where $L_m \gg L_r$, thus the primary current during the freewheeling operation will only change slightly, and can be approximated to be unchanged for simplicity. The equivalent circuits of the freewheeling operation in both halves of the switching cycle are shown in Figure 2.7 and Figure 2.8.

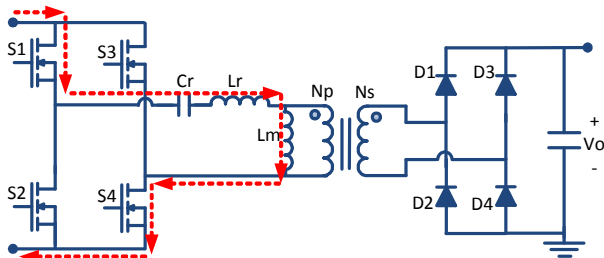


Figure 2.7

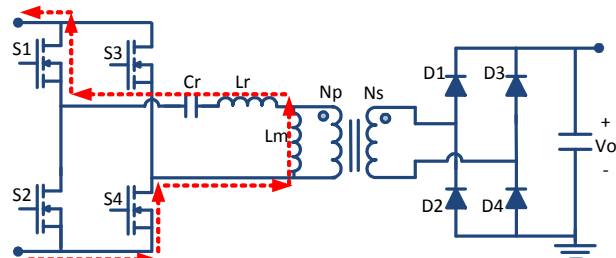


Figure 2.8

Table 1 explains the converter modes of operation and shows key waveforms

Table 1

| At Resonant frequency operation $fs=fr$. | Above resonant frequency operation $fs>fr$. | Below resonant frequency operation $fs<fr$ |
|--|--|--|
| <p>Each half of the switching cycle contains a complete power delivery operation (described above), where the resonant half cycle is completed during the switching half cycle.</p> <p>By end of the switching half cycle, the resonant inductor current I_{Lr} reaches the magnetizing current I_{Lm}, and the rectifier current reaches zero.</p> <p>The resonant tank has unity gain and best optimized operation and efficiency, therefore, transformer turns ratio is designed such that the converter operates at this point at nominal input and output voltages.</p> | <p>Each half of the switching cycle contains a partial power delivery operation (described above), similar to the resonant frequency operation, but it differs in that the resonant half cycle is not completed and interrupted by the start of the other half of the switching cycle, hence primary side MOSFETs have increased turn off losses and secondary rectifier diodes have hard commutation.</p> <p>The converter operates in this mode at higher input voltage, where a step down gain or buck operation is required.</p> | <p>Each half of the switching cycle contains a power delivery operation (described above), at the time when resonant half cycle is completed and resonant inductor current I_{Lr} reaches the magnetizing current, the freewheeling operation (as described above) starts and carries on to the end of the switching half cycle, hence primary side have increased conduction losses due to the circulating energy.</p> <p>The converter operates in this mode at lower input voltage, where a step up gain or boost operation is required.</p> |
| <p>Key waveforms for the $fs=fr$ mode include the drain-to-source voltage $V_{ds_S2,S3}$, resonant inductor current I_{Lr}, and antiparallel diode currents $I_{D1,D4}$ and $I_{D2,D3}$. The period $T_s = 1/fs$ is indicated.</p> | <p>Key waveforms for the $fs > fr$ mode show the same parameters as the $fs=fr$ mode, but with the characteristic interruption of the resonant half-cycle by the start of the next switching half-cycle.</p> | <p>Key waveforms for the $fs < fr$ mode show the resonant inductor current I_{Lr} rising to the magnetizing current I_{Lm} during the switching half-cycle, followed by a freewheeling period where the current decays.</p> |

3 Design Steps

This section is to explain the impact of design parameters on voltage regulation and efficiency performance, and facilitate the design and selection of such parameters. Our ultimate design objective is to achieve the best performance while reaching the gain requirement for all line and load conditions. And for safe operation, we must determine the minimum switching frequency the controller shall limit in order to maintain the operation in the inductive region.

The following are detailed explanation of all design steps; additionally Figure 3.1 shows a design flow chart that summarizes the design methodology.

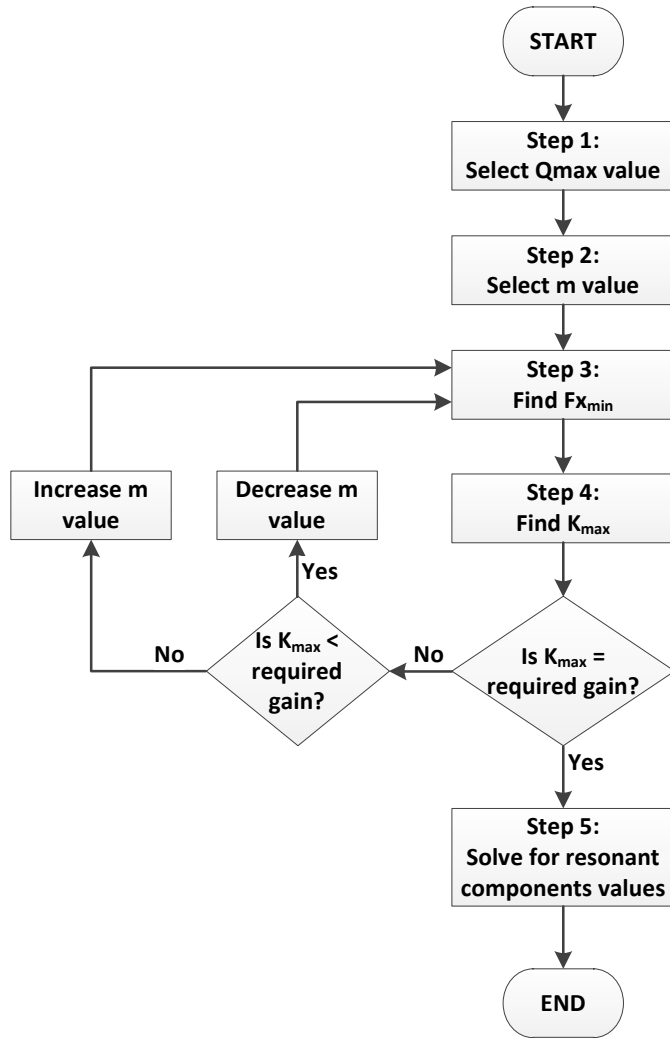


Figure 3.1 Design flow chart

Step 1: Selecting the Qmax Value

Quality factor $Q = \frac{\sqrt{L_r/C_r}}{R_{ac}}$ depends on the load current. Heavy load conditions operate at high Q values, while lighter loads have lower Q values. It is important to set a value for the Qmax associated with the maximum load point.

To illustrate the effect of the Q value on voltage regulation, Figure 3.2 shows an example voltage gain plot for different Q values. Let's assume that the resonant tank gain is required to range from 0.8 to 1.2 for example, we can see that the low Q value curve ($Q=0.3$) can reach higher boost gain, but it is less sensitive to frequency modulation in the "above resonance $f_s > f_r$ " region, hence, switching frequency has to increase much in order to reach the minimum voltage gain ($K=0.8$), causing extra switching losses, while the higher Q

value curve ($Q=1$) can reach the minimum gain ($K=0.8$) with less switching frequency increase, but unable to reach the maximum gain ($K=1.2$). Therefore, a moderate Q value of around 0.5 seems to satisfy the voltage gain requirement in this specific case.

We conclude that adjusting the Q value can help achieving the maximum gain but increases the frequency modulation range, thus, we should not rely on tuning the Q_{max} value as a design iteration in order to reach the desired maximum voltage gain, but instead we should rely on tuning the m value as will be explained in the next step.

Although there isn't a direct method for selecting the optimum Q value, we should select Q_{max} moderately as discussed earlier and based on the specific design in hand.

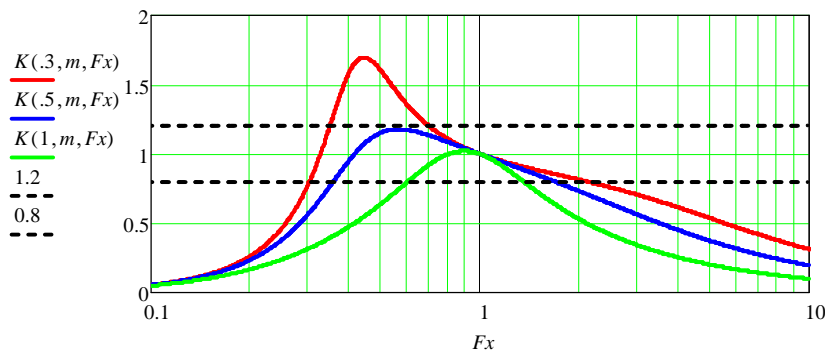


Figure 3.2

Step 2: Selecting the m Value

As mentioned above, $m = \frac{L_r + L_m}{L_r}$, m is a static parameter that we have to start the design by optimizing its

value, therefore it's important to understand the impact of the m ratio on the converter operation. To illustrate the effect of the m value, Figure 3.3 shows the same resonant tank gain plots but for different m values, $m=3, 6$ and 12 . It is obvious that lower values of m can achieve higher boost gain, in addition to the narrower range of the frequency modulation, meaning more flexible control and regulation, which is valuable in applications with wide input voltage range. Nevertheless, low values of m for the same quality factor Q and resonant frequency f_r means smaller magnetizing inductance L_m , hence, higher magnetizing peak-peak current ripple, causing increased circulating energy and conduction losses.

We have to start by selecting a reasonable initial value for m (6-10), and then optimize it by few iterations to get the maximum m value that can still achieve the maximum gain requirement for all load conditions.

Low m value:

- Higher boost gain
- Narrower frequency range
- **More flexible regulation**

High m value:

- Higher magnetizing inductance
- Lower magnetizing circulating current
- **Higher efficiency**

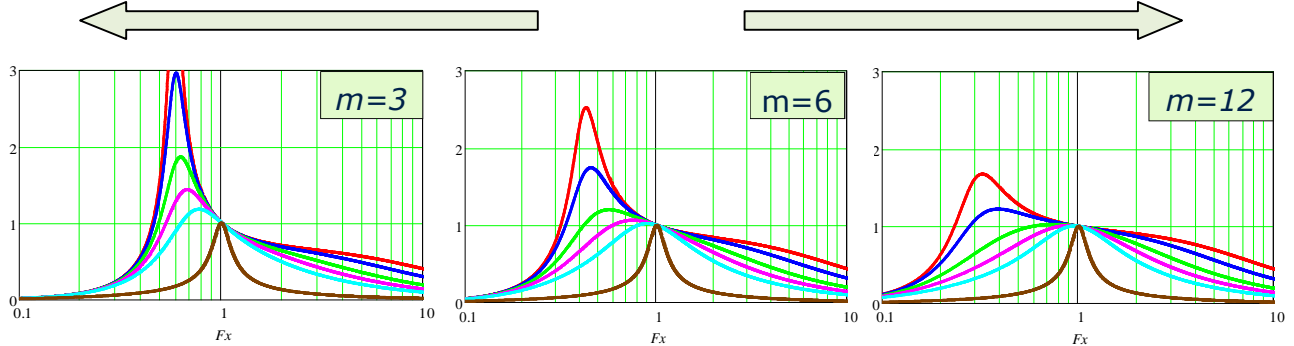


Figure 3.3

Step 3: Finding the Minimum Normalized Switching Frequency

After selecting a value for Qmax and an initial value for m, we need to find the minimum normalized switching frequency that will guarantee inductive operation for the Qmax (max load) condition, this minimum frequency will also guarantee inductive operation for all other loads.

The minimum normalized switching frequency occurs at the peak gain of the Qmax curve, so it can be found by solving Eq. 2 (assumed Qmax=0.4 and m=6 as an example), or can be visually spotted in the gain plot as in Figure 3.4.

$$\frac{d}{dF_x} K(Q, m, F_x) \Big|_{Q_{\max}=0.4, m=6} = 0 \quad \text{Eq. 2}$$

→ Solve for F_x_{\min}

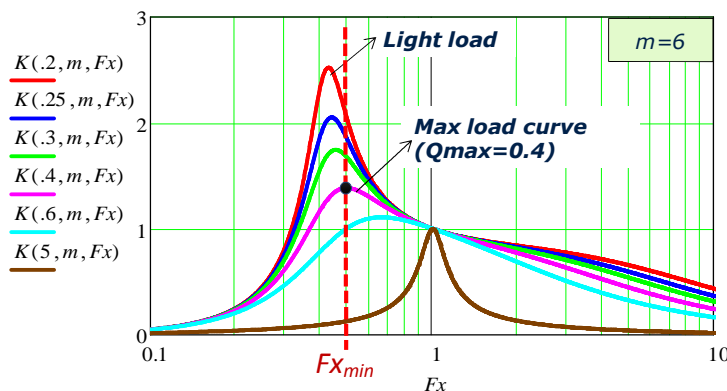


Figure 3.4

Step 4: Voltage Gain Verification

This step is to verify that the maximum gain K_{\max} reached during maximum load by the selected m value is adequate. This can be done by solving Eq. 3, or can be visually spotted in the gain plot as in Figure 3.4.

$$K_{\max} = K(Q_{\max}, m, F_x) \quad \text{Eq. 3}$$

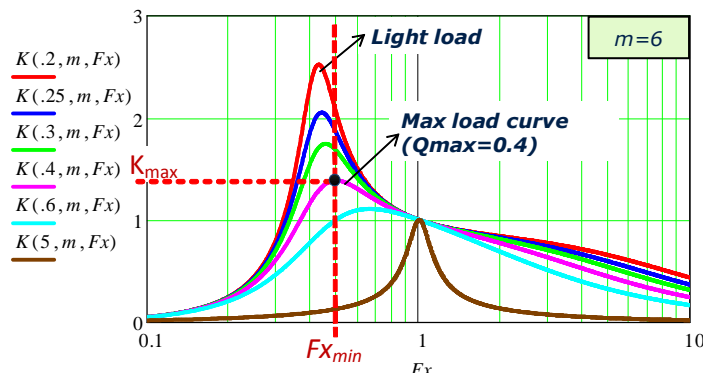


Figure 3.5

Few iterations are needed in order to reach the optimized design, as shown in the design flow chart in Figure 3.1. If K_{\max} is not enough, then we have to reduce the m value and repeat steps 3 and 4, in order to gain a higher boost gain. On the other side, If K_{\max} is higher than what is required; in that case we can increase the m value and repeat steps 3 and 4 in order to gain a better efficiency.

Step 5: Calculating Resonant Components Values

After few iterations of the design flow and reaching the optimum m value, we can proceed to calculating the resonant tank components values, Eq. 4 and Eq. 5 can be solved to find L_r and C_r , and then L_m can be calculated using Eq. 6.

$$R_{ac,min} = \frac{8}{\pi^2} \cdot \frac{N_p^2}{N_s^2} \cdot \frac{V_o^2}{P_{o,max}}$$

$$Q_{\max} = \frac{\sqrt{L_r/C_r}}{R_{ac,min}} \quad \text{Eq. 4}$$

$$f_r = \frac{1}{2\pi\sqrt{L_r C_r}} \quad \text{Eq. 5}$$

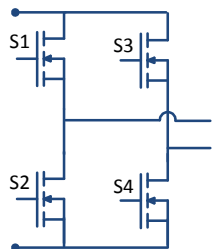
$$m = \frac{L_r + L_m}{L_r} \quad \text{Eq. 6}$$

It must be noted that selection of the resonant frequency f_r was not considered in the design steps above, since it has no impact on the maximum gain and operation region of the resonant converter, however it is selected considering the converter power density and power losses.

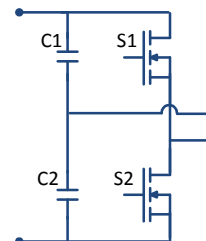
4 Bridge and Rectifier Selection

An important step to achieve the best converter performance is to choose the right bridge and rectifier circuits.

LLC converters can be implemented with a full-bridge or a half-bridge circuit on the primary side, as shown in Figure 4.1,



Full-bridge switching circuit



Half-bridge switching circuit

Figure 4.1

Table 2 shows a comparison between the half-bridge and the full-bridge switching circuits.

A half-bridge would have twice the current of what a full-bridge would have, the squared rms current in the half-bridge case is four times, the number of switches in a half bridge is half of that in a full-bridge, therefore, the total FETs conduction losses of a half-bridge is twice compared to the full-bridge.

Although a half-bridge requires half the primary number of turns for the same voltage gain and magnetic flux swing, thus half the primary winding resistance, the primary copper losses are still twice compared to the full-bridge because the squared rms current in the half-bridge case is four times.

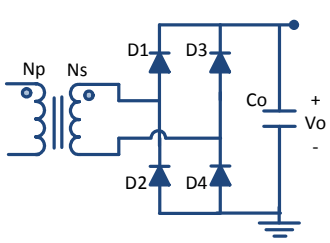
So in applications with high primary currents, where conduction losses are dominant, it is suggested to use a full-bridge switching circuit.

Table 2

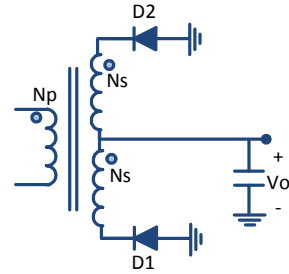
| Primary Bridge - Half-Bridge compared to Full-Bridge | | | | | | |
|---|-------------|----------------|------------------------------|----------|-----------|---------------------------------|
| I_{rms} | I_{rms}^2 | Number of FETs | Total FETs conduction losses | N_p | R_{pri} | Transformer primary copper loss |
| $\times 2$ | $\times 4$ | $\div 2$ | $\times 2$ | $\div 2$ | $\div 2$ | $\times 2$ |

*Comparison assumes same FET and same transformer core

LLC converters can also be implemented with a full-bridge or a full-wave rectifier circuit on the secondary side, as shown in Figure 4.2



Full-bridge rectifier



Full-wave rectifier

Figure 4.2

Table 3 shows a comparison between the full-bridge and full-wave rectifiers.

A full-wave rectifier requires diodes that are twice the voltage rating compared to a full-bridge rectifier, but it has only two diodes while the full-bridge rectifier has four diodes, since each diode in both rectifier circuits carries the same average current, the full-wave rectifier has half the total diode conduction losses compared to the full-bridge rectifier.

A full-wave rectifier has two secondary windings, hence the resistance is doubled for the same winding area, each winding in a full-wave carries an rms current that is $\sqrt{0.5}$ of the rms current of the full-bridge circuit, therefore the total secondary windings copper losses of the full-wave rectifier is twice compared to the full-bridge rectifier.

In applications with high output voltages, the full bridge rectifier is advantageous since we can use diodes with half the voltage rating compared to the full-wave rectifier. While in low output voltages and high currents application, the full-wave is more common, because of lower total conduction losses and lower component count and cost.

Table 3

| Secondary Rectifier - Full-Wave compared to Full-Bridge | | | | | | |
|--|------------------|-------------------------|------------------------------|-----------------------|-----------------------|-----------------------------------|
| Diode voltage rating | Number of diodes | Diode conduction losses | Number of secondary windings | R_{sec} per winding | I_{rms} per winding | Transformer secondary copper loss |
| $\times 2$ | $\div 2$ | $\div 2$ | $\times 2$ | $\times 2$ | $\times \sqrt{0.5}$ | $\times 2$ |

*Comparison assumes same diode voltage drop and same transformer core

5 Design Example

5.1 Application and Specifications

Our design example is applicable to the dc-dc stage of a solar micro inverter, as shown in Figure 5.1, with specifications as listed in Table 4. According to the discussion in section 4, the LLC converter will be implemented with a full-bridge on the primary side and a full-bridge rectifier on the secondary side, same circuit as shown in Figure 2.1.

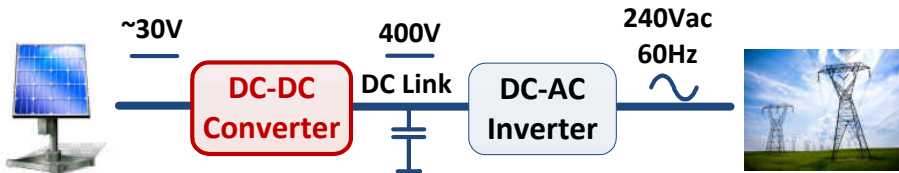


Figure 5.1

Table 4 Specifications

| | |
|--|-------------------------|
| Output voltage | 400V |
| Input voltage | 18V – 36V (33V nominal) |
| Output power | 250W |
| <i>Output power derates linearly with input voltage Ex: Output power= 125W @ Vin=18V</i> | |
| Resonant frequency | 100kHz |

5.2 Design Steps

We start the design by calculating the transformer turn ratio and the minimum and maximum voltage gains of the resonant tank, as follows.

$$M_{nom} = 1$$

$$\frac{N_p}{N_s} = \frac{V_{in_nom}}{V_{out}} \cdot M_{nom} \rightarrow \frac{N_p}{N_s} = 0.0825$$

$$M_{max} = \frac{V_{in_nom}}{V_{in_min}} \cdot M_{nom} \rightarrow M_{max} = 1.833$$

$$M_{min} = \frac{V_{in_nom}}{V_{in_max}} \cdot M_{nom} \rightarrow M_{min} = 0.917$$

Next, we follow the design steps discussed in section 3, as follows.

Step 1: Selecting the Qmax Value

Let's choose $Q_{max} = 0.4$

Step 2: Selecting the m Value

Let's choose $m = 6.3$

Step 3: Finding the Minimum Normalized Switching Frequency

We can solve the gain equation to find the minimum frequency, which occurs at the peak of the Qmax curve, as shown below, or we can look it up from the gain plot as shown in Figure 5.2.

$$\frac{d}{dF_X} K(Q_{max}, m, F_{Xmin}) \Big|_{Q_{max}=0.4, m=6.3} = 0 \rightarrow F_{Xmin} = 0.489$$

$$\rightarrow f_{s_min} = F_{Xmin} \cdot f_r = 48.9 \text{ kHz}$$

Step 4: Voltage Gain Verification

Since the power is derated at lower input voltages as listed in the specifications, we have to calculate the maximum Q value at the minimum input voltage case ($Q_{max@Vmin}$), as follows. Note that this power derating specification is related to the solar panel I-V characteristics. (In case of other applications where power rating is the same across the input voltage range, we only have a single Q_{max} value).

$$Q_{max@Vmin} = Q_{max} \cdot \frac{V_{in_min}}{V_{in_max}} = 0.2$$

Then we can calculate the maximum gain reached at the minimum switching frequency for the $Q_{max@Vmin}$ condition, or we can look it up from the gain plot as shown in Figure 5.2.

$$K_{max} = K(Q_{max@Vmin}, m, F_{Xmin}) = 1.974$$

$K_{max} = 1.974 > M_{max} = 1.833 \rightarrow$ No need for tuning the m value

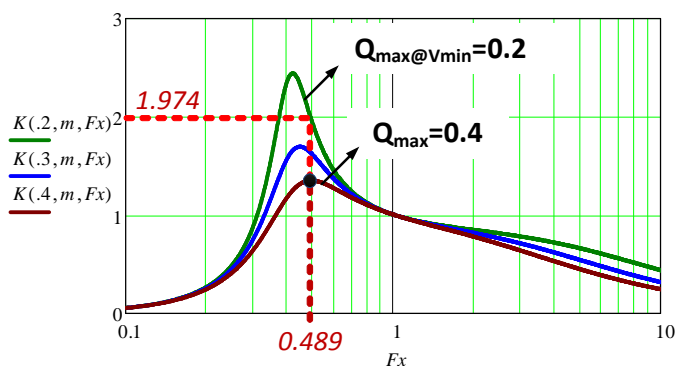


Figure 5.2

Step 5: Calculating Resonant Components Values

The reflected load resistance at full load is,

$$R_{ac_min} = \frac{8}{\pi^2} \cdot \left(\frac{N_p}{N_s}\right)^2 \frac{V_{out}^2}{P_{o,max}} \rightarrow R_{ac_min} = 3.534 \Omega$$

Next we solve the equations below to obtain the resonant tank components values

$$Q_{max} = 0.4 = \frac{\sqrt{L_r/C_r}}{3.534 \Omega}$$

$$f_r = 100 \text{ kHz} = \frac{1}{2\pi\sqrt{L_r \cdot C_r}}$$

$$m = 6.3 = \frac{L_r + L_m}{L_r}$$

$$\therefore L_r = 2.25 \mu H \quad L_m = 11.93 \mu H \quad C_r = 1.13 \mu F$$

5.3 Experimental Waveforms and Efficiency

The design example was implemented with the specification shown in Table 5

Table 5 Prototype specifications

| | |
|--|--------------|
| Resonant frequency f_r | 110 kHz |
| Minimum switching frequency f_{s_min} | 50 kHz |
| Resonant capacitor C_r | 0.94 μ F |
| Transformer Specifications | |
| Turns ratio $N_p:N_s$ | 1:12 |
| Leakage (Resonant) inductor L_r | 2.2 μ H |
| Magnetizing inductor L_m | 12.2 μ H |

Figure 5.3 through Figure 5.6 shows experimental waveforms at different input voltage conditions,

Red channel: Primary FET V_{gs}

Yellow channel: Primary FET V_{ds}

Green channel: Resonant current I_{Lr}

Blue channel: Rectifier output current $I_{D1}+I_{D3}$

Figure 5.3

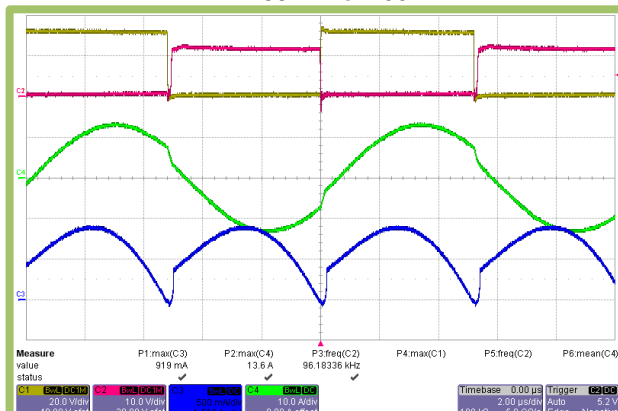


Figure 5.4

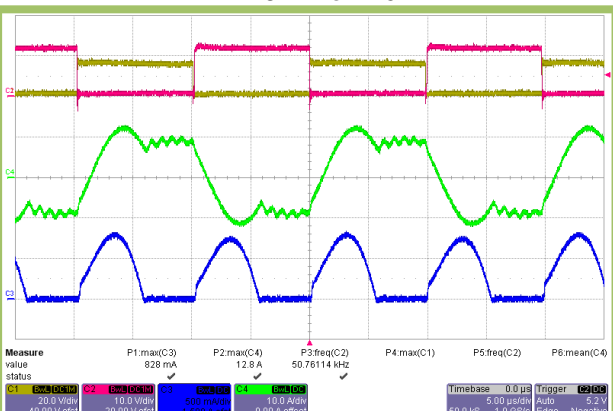


Figure 5.5

Figure 5.6

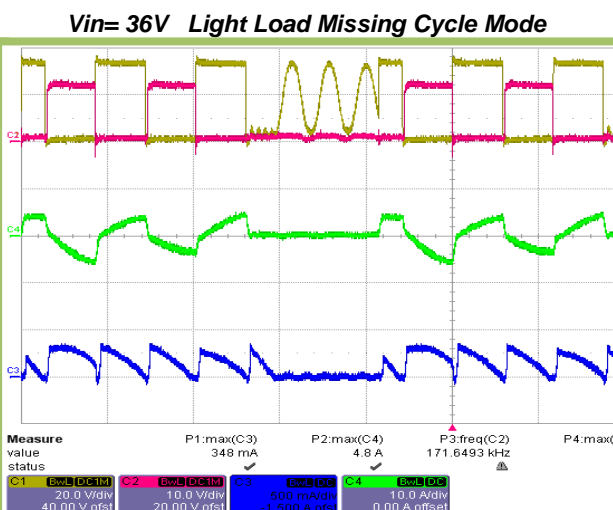
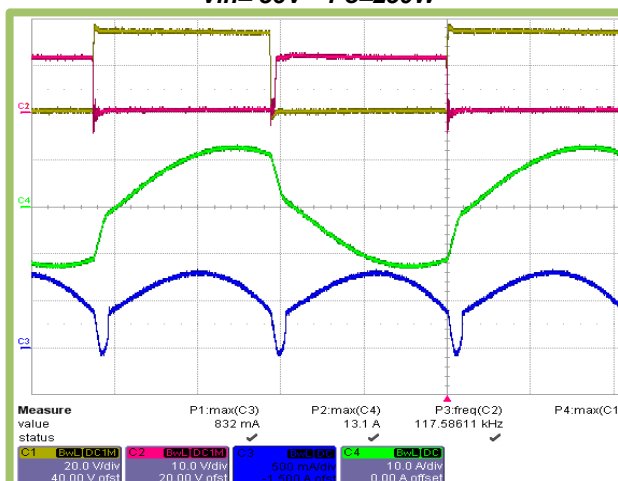
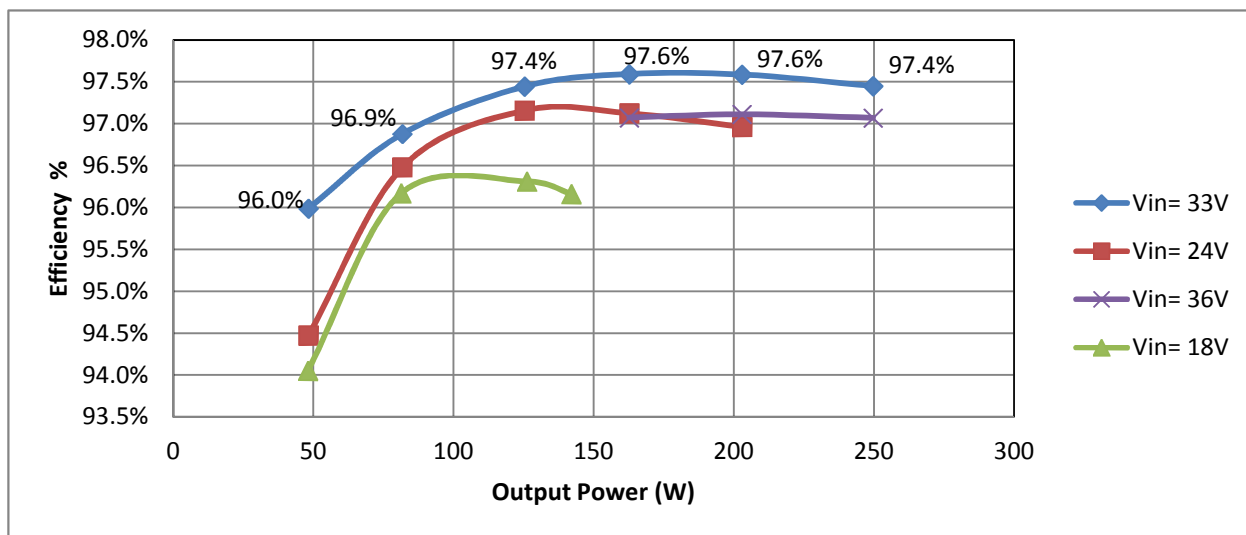


Figure 5.6

Table 6 Efficency data

| Input Voltage | Output Power (% of 250W) | | | | |
|---------------|--------------------------|---------|-------|-------|-------|
| | 20% | 40% | 60% | 80% | 100% |
| 36V | 97.1% ** | 97.1%** | 97.1% | 97.1% | 97.1% |
| 33V | 96.0% | 97.2% | 97.6% | 97.6% | 97.4% |
| 24V | 94.5% | 96.8% | 97.1% | 97.0% | |
| 18V | 94.0% | 96.3% | 96.2% | | |

** Missing cycle mode / Burst mode operation

**Figure 5.7 Efficiency curves**

6 Schematics and Bill of Material

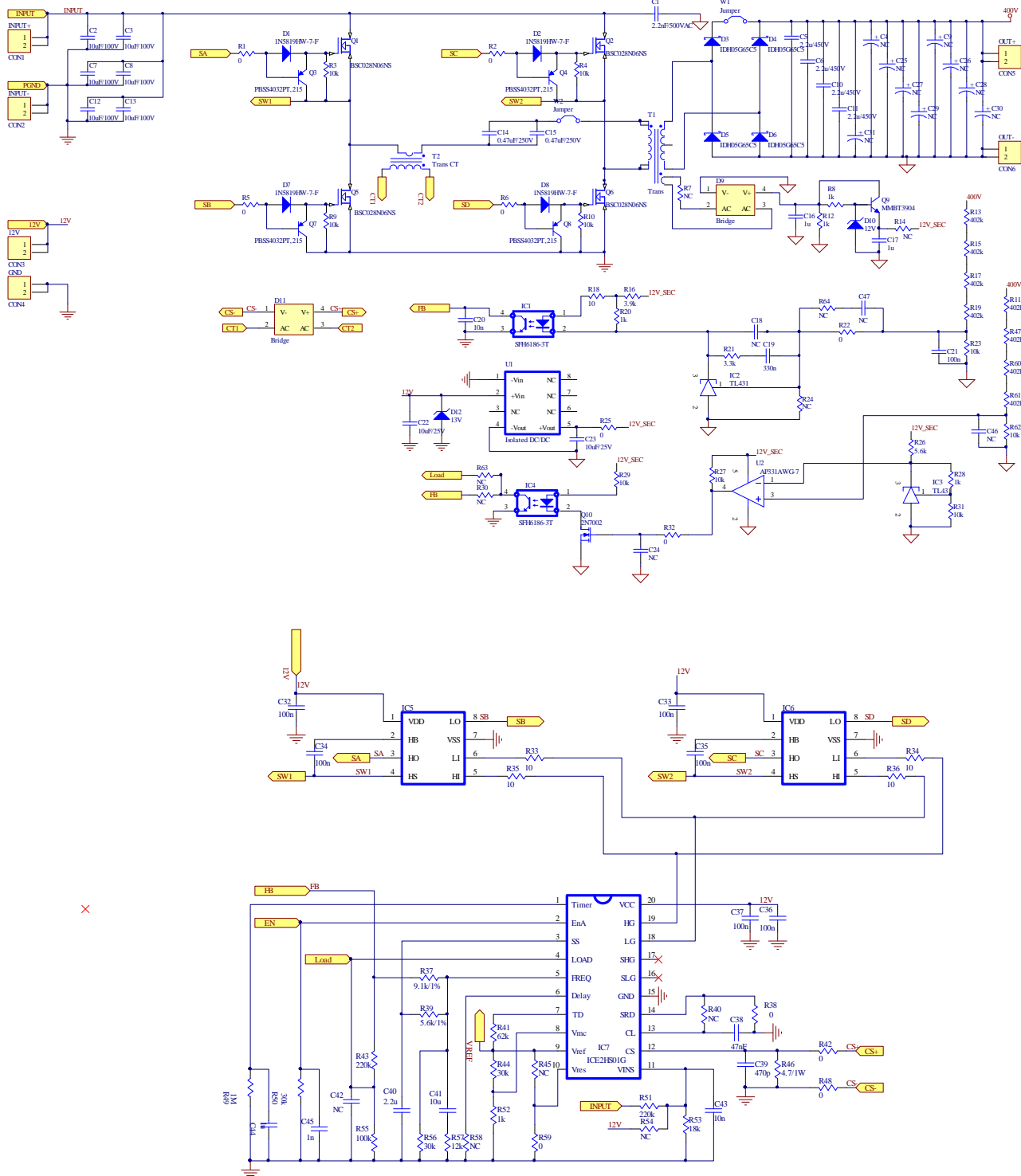


Figure 6.1 Schematics

Table 7 Bill of Material

| Qty | Designator | Value | Part Number |
|-----|--|----------------|---------------------|
| 1 | C1 | 2.2nF/500VAC | VY1222M47Y5UQ63V0 |
| 6 | C2, C3, C7, C8, C12, C13 | 10uF/100V | C5750X7S2A106M |
| 9 | C4, C9, C25, C26, C27, C28, C29, C30, C31 | NC | |
| 4 | C5, C6, C10, C11 | 2.2u/450V | B32674D4225K |
| 2 | C14, C15 | 0.47uF/250V | B32652A3474J |
| 3 | C16, C17, C44 | 1u | C3216X7R1H105K |
| 15 | C18, C24, C42, C46, C47, R7, R14, R24, R30, R40, R45, R54, R58, R63, R64 | NC | |
| 1 | C19 | 330n | GRM319R71H334KA01D |
| 2 | C20, C43 | 10n | GRM319R71H103KA01D |
| 7 | C21, C32, C33, C34, C35, C36, C37 | 100n | GRM319R71H104KA01D |
| 2 | C22, C23 | 10uF/25V | TMK316B7106KL-TD |
| 1 | C38 | 47nF | GRM31M5C1H473JA01L |
| 1 | C39 | 470p | CC1206KRX7R9BB471 |
| 1 | C40 | 2.2u | C3216Y5V1H225Z/0.85 |
| 1 | C41 | 10u | TMK316B7106KL-TD |
| 1 | C45 | 1n | GRM3195C1H102JA01D |
| 4 | D1, D2, D7, D8 | BAS 3010A | BAS 3010A-03W E6327 |
| 4 | D3, D4, D5, D6 | IDH05G65C5 | IDH05G65C5 |
| 2 | D9, D11 | Bridge | BAS3007A-RPP |
| 1 | D10 | 12V | SMAZ12-TP |
| 1 | D12 | 13V | 3SMAJ5928B-TP |
| 2 | IC1, IC4 | SFH6186-3T | SFH6186-3T |
| 2 | IC2, IC3 | TL431 | TL431CPK |
| 2 | IC5, IC6 | SO8 | LM5100AM/NOPB |
| 1 | IC7 | ICE2HS01G | ICE2HS01G |
| 4 | Q1, Q2, Q5, Q6 | BSC028N06NS | BSC028N06NS |
| 4 | Q3, Q4, Q7, Q8 | PBSS4032PT,215 | PBSS4032PT,215 |
| 1 | Q9 | MMBT3904 | MMBT3904FSCT-ND |
| 1 | Q10 | 2N7002 | 2N7002 L6327 |
| 11 | R1, R2, R5, R6, R22, R25, R32, R38, R42, R48, R59 | 0 | ERJ-8GEY0R00V |
| 9 | R3, R4, R9, R10, R23, R27, R29, R31, R62 | 10k | ERJ-8ENF1002V |
| 5 | R8, R12, R20, R28, R52 | 1k | ERJ-8GEYJ102V |
| 8 | R11, R13, R15, R17, R19, R47, R60, R61 | 402k | ERJ-8ENF4023V |
| 1 | R16 | 3.9k | ERJ-8GEYJ392V |
| 5 | R18, R33, R34, R35, R36 | 10 | ERJ-8GEYJ100V |
| 1 | R21 | 3.3k | ERJ-8GEYJ332V |
| 1 | R26 | 5.6k | ERJ-8ENF5601V |
| 1 | R37 | 9.1k/1% | ERJ-8ENF9101V |
| 1 | R39 | 5.6k/1% | ERJ-8ENF5601V |
| 1 | R41 | 62k | ERJ-8ENF6202V |
| 2 | R43, R51 | 220k | ERJ-8ENF2203V |
| 3 | R44, R50, R56 | 30k | ERJ-8ENF3002V |
| 1 | R46 | 4.7/1W | ERJ-1TRQF4R7U |
| 1 | R49 | 1M | ERJ-8ENF1004V |
| 1 | R53 | 18k | ERJ-8ENF1802V |
| 1 | R55 | 100k | ERJ-8ENF1003V |
| 1 | R57 | 12k | ERJ-8ENF1202V |
| 1 | T1 | Transformer | Custom** |
| 1 | T2 | Trans CT | B82801B504A50 |
| 1 | U1 | Isolated DC/DC | VBT1-S12-S12-SMT |
| 1 | U2 | AP331AWG-7 | AP331AWG-7 |

**Transformer built by Midcom-Wurth Electronics, E41/17/12-3C90

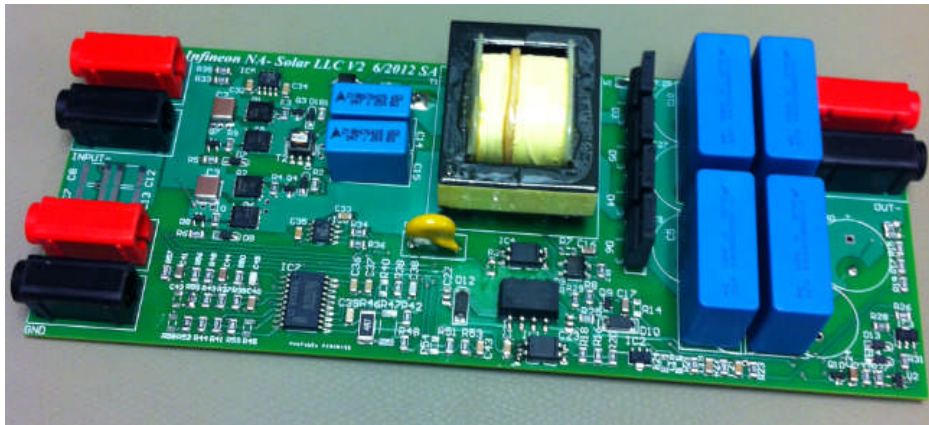


Figure 6.2

7 References

- [1] Infineon Technologies: ICE2HS01G datasheet, High Performance Resonant Mode Controller, V1.1, August 2011.
- [2] Infineon Technologies: Design Guide for LLC Converter with ICE2HS01G, V1.0, July 2011.
- [3] Infineon Technologies: 300W LLC Evaluation Board with LLC controller ICE2HS01G, V1.1, August 2011.